

Fourier-transform-EPR and low-frequency-EPR studies of nitroxides

M. K. Bowman¹, T. J. Michalski¹, M. Peric², and H. J. Halpern²

¹Chemistry Division, Argonne National Laboratory, Argonne, IL 60439 USA

²University of Chicago Medical Center, Chicago, IL 60637 USA

Abstract - The nitroxide spin labels are a class of stable free radicals that have wide applications as probes of chemical and biological systems in electron paramagnetic resonance (EPR) experiments. Measurements of the concentration of paramagnetic species and of rotational or translational motion can be made using the relaxation times and the lineshape of the nitroxide probe. In the fast motional limit, the relaxation times are easily obtained from the conventional EPR spectrum if inhomogeneous broadening from the unresolved hyperfine couplings is not too great. Pulsed and Fourier-Transform EPR (FT-EPR) methods allow the measurements independent of inhomogeneous broadening. In biological studies involving large aqueous samples, it is advantageous to use low-frequency EPR (LF-EPR) near 250 MHz to reduce microwave absorption from the sample. The nitroxide spin-label probes are as effective in LF-EPR as in the usual X-band EPR.

INTRODUCTION

Nitroxide spin labels have long been used as probes of the static and dynamic properties of chemical and biological systems. They are relatively stable free radicals which are easily detected using EPR spectroscopy. Their most important characteristic for use as a probe is the sensitivity of their EPR spectra to their environment. This sensitivity appears in both the continuous-wave (CW) EPR spectra as changes in spectral shape and in time-domain or pulsed EPR spectra as changes in the relaxation times. These are complimentary views of the same spin dynamics. Both methodologies have been used to study a wide range of systems.

A detailed comparison of EPR lineshapes from CW-EPR and the spin-spin relaxation rate T_2^{-1} from electron spin echo measurements found that the two methods give equivalent results in non-viscous liquids, ref. 1. The rotational correlation times and the spin exchange rates from collisions between two nitroxide molecules were evaluated. The spin label was deuterated to minimize inhomogeneous broadening for the CW-EPR. However, proton impurities in the spin label seemed to affect the spin exchange measurements in CW-EPR but not in pulsed EPR. CW-EPR is a convenient technique in the fast motional limit when inhomogeneous broadening is small. The development of very efficient, parametric methods for decomposing lineshapes into homogeneous and inhomogeneous contributions, ref. 2, has eliminated the need for complex lineshape simulations. However, when inhomogeneous broadening is large, the ability of pulsed EPR to isolate and measure T_2 is needed.

In the slow motional regime, the agreement between CW and pulsed EPR measurements has not been as good, refs. 3,4,5,6. The discrepancies seem to arise from the greater sensitivity of pulsed measurements to the detailed motion of the spin label. CW-EPR, including variations such as saturation-transfer, often produce spectra which can be fit equally well by several models of spin-label motion. In experiments on spin-labelled sickle-cell hemoglobin, ref. 6, pulsed EPR found differences between hemoglobin immobilized by different methods while CW-EPR methods gave identical spectra. In FT-EPR experiments, sickle-cell hemoglobin gels, at physiological concentrations and temperatures, showed motion that was not adequately described by any of the motional models proposed on the basis of CW-EPR lineshape and saturation transfer experiments.

Pulsed EPR measurements seem to be more sensitive than CW-EPR to the detailed interaction of a spin label with its environments in the "slow motional" regime where product of the rotational correlation time, t_r , and the anisotropy of the spectrum, ω , is large, i.e. $\omega t_r > 1$. On the other hand, in the "fast motional" limit, $\omega t_r < 1$, CW and pulsed EPR give equivalent results but not necessarily equivalent convenience. Pulsed EPR has the advantage that the pulse sequence can be tailored to cleanly measure one property of a spin system at a time, so that a number of measurements produces a very accurate and detailed picture. CW-EPR, on the other hand, produces spectra which depend on several parameters. Accurately separating those different parameters can be difficult if not impossible.

EPR is called upon to answer more detailed questions about increasingly more complex systems; consequently, measurements are being made under more extreme conditions. An example is the renewed interest in EPR at low frequencies and fields for the measurement of lossy or conductive samples and for *in vivo* spectroscopy. Such drastic changes in frequency could affect the sensitivity and usefulness of nitroxides as probes because the high-field approximation is no longer valid and rotational times far exceed the EPR frequency. We focus here on a comparison of LF-EPR at 250 MHz and FT-EPR at 9100 MHz on nitroxides in non-viscous solution. We compare the effects of spin exchange on two novel nitroxides.

LINewidth AND RELAXATION RATES

Recent FT-EPR experiments on laser-induced, electron-transfer reactions of chlorophyll and quinones, refs. 7,8, involve the transport properties of chlorophyll in solution. We have synthesized a spin-labelled derivative of chlorophyll for EPR measurements of spin exchange rates driven by translational diffusion. A nitroxide derivative **3**, Fig. 1, was synthesized with a shorter link than those described earlier, ref. 9. To a solution of pyropheo-

phorbide **a**, 15 mg in 7 ml of dry CH_2Cl_2 and 50 μl of 1,4-butanediol, 1,3-dicyclohexylcarbodiimide, 10 mg in 4 ml of CH_2Cl_2 , was added. Reaction was terminated after 3 hours when 90% of pyropheophorbide **a** reacted, as determined by TLC. Methylene chloride (40 ml) was added followed by washes with water (3x10 ml). Removal of solvent under reduced pressure and then isolation of product by HPLC [ODS, SiO_2 , 1 cm x 25 cm, flow rate: 1 ml/min, $\text{CH}_2\text{Cl}_2/\text{CH}_3\text{CO}_2\text{CH}_2\text{CH}_3$, 92/8, (v/v), resulted in the preparation of 8.5 mg of ^{17}O -Hydroxybutoxy pyropheophorbide **a** (**1**). ^{252}Cf PDMS: $[\text{M}^*] = 606.47$ and $^1\text{H-NMR}$ confirmed the product. To the solution of 6 mg of **1** in 4 ml of dry CH_2Cl_2 , 4 mg of 1,3-dicyclohexylcarbodiimide and 2 mg in 4 ml of CH_2Cl_2 , were added. Reaction was terminated after 4 hours. After isolation, 5 mg of **2** was collected as a dark brown solid. Structure of the product was confirmed by ^{252}Cf PDMS: $[\text{M}^*]$ (obs) = 774.84, EPR and visible spectroscopy.

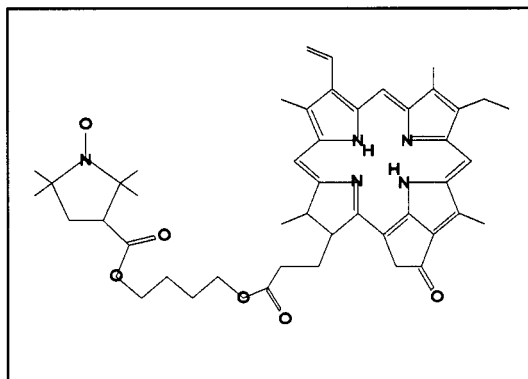


Fig. 1 Structure of ^{17}O -(3-Carboxy-2,2,5,5-Tetramethyl-1-pyrrolidinyloxy-butoxy)1-pyropheophorbide **a**, **2**.

Degassed solutions of **2** in ethanol were prepared in 4 mm diameter, quartz EPR tubes and sealed. The same samples were measured at room temperature using FT-EPR with the spectrometer described in refs. 10,11 and using LF-EPR using the spectrometer described in ref. 12. The pulsed measurements used two microwave pulses to generate an electron spin echo from the samples. The echo shape was Fourier transformed to give the intensity of the central nitrogen hyperfine line. No proton hyperfine couplings were observable. The line intensity was measured as a function of the time τ between the two pulses. The intensity decayed exponentially with a rate constant determined by T_2^{-1} . The concentration dependence of the spin-spin relaxation rate T_2^{-1} is shown in Fig. 2. LF-EPR spectra of the same samples were fit, using a non-linear, least-squares procedure, by the sum of a gaussian and lorentzian lineshape. This sum is a very good approximation to the Voigt lineshape expected from the inhomogeneously-broadened lines from **2** and is very easy to calculate, ref. 2. The lorentzian linewidth, i.e., the T_2^{-1} , was calculated from the fit parameters using the formulas of Bales, ref. 2, and are plotted in Fig. 2.

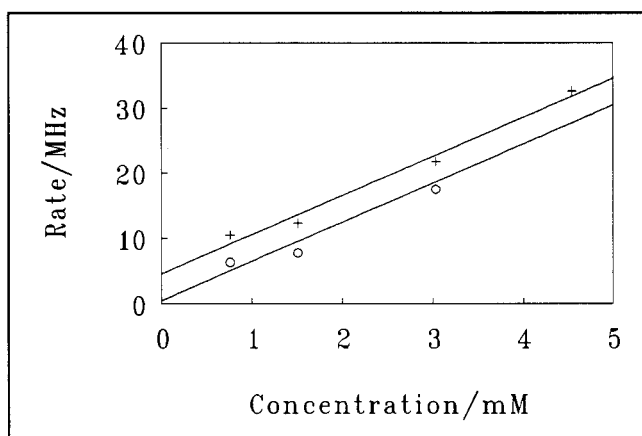


Fig. 2 Dependence of the spin-spin relaxation rate, T_2^{-1} , on the concentration of compound **II** in degassed ethanol at room temperature. + LF-EPR, o FT-EPR measurements. The solid lines are linear fits to the data.

The concentration dependence of the relaxation rates for **2** have the same slope but different intercepts for the two methods. The solid lines on Fig. 2 have a common slope of $6.00 \times 10^9 \text{ M}^{-1}\text{s}^{-1}$, but intercepts of 0.50 MHz for the FT-EPR measurements at X-band and 4.59 MHz for the LF-EPR at 250 MHz. The two measurements even have similar deviations from the fitted lines suggesting that they reflect small deviations in sample concentration rather than measurement error. Note that the intercept, or intrinsic spin-spin relaxation rate, is larger at the lower frequency and field where the g-factor anisotropy contributes less to the relaxation.

Nitroxide **3**, Fig. 3, has been developed as a probe molecule for *in vivo* oximetry and its synthesis is detailed in ref. 13. Its use in spin-label oximetry relies on the measurement of spin exchange rates between molecular oxygen in solution and the spin label. Molecular oxygen has a paramagnetic, triplet ground state and produces spin-exchange broadening like any free radical. The diffusion coefficient of oxygen *in vivo* is constant, so that the spin-exchange rate is a measure of the oxygen concentration around the spin label. This application has been well established at X-band, refs. 14,15,16 and is now being applied at other EPR frequencies. In oximetric applications, the spin label is sensitive to spin exchange with oxygen as well as with itself at the millimolar spin-label concentrations used for *in vivo* experiments. Thus, some correction must be made for spin-exchange with other spin-label molecules.

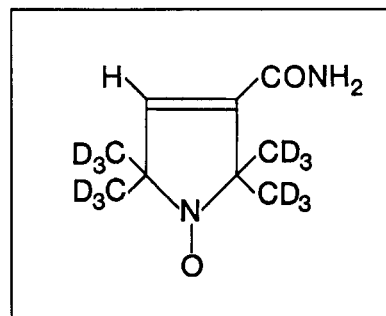


Fig. 3 4-hydro-3-carbamoyl-2,2,5,5-tetra(perdeutero-methyl)pyrrolin-1-yloxy, **3**.

The use of LF-EPR is necessary for whole-animal oximetry for two reasons. First, most animal subjects are much larger than the wavelength of X-band microwaves and second, tissue simply absorbs too much microwaves for any internal oximetric measurements. Operation at 250 MHz overcomes both problems. However, an additional problem, that of correcting for spin exchange with other spin-label molecules, remains. It is not sufficient to measure the average concentration of spin label since it may be distributed very non-uniformly in an animal. **3** was designed specifically to solve that problem. It is deuterated except at the 4-position where the proton hyperfine coupling is largest. This produces a spin label with a six line spectrum, Fig. 4, a triplet from the nitrogen

split into doublets by the remaining proton. This spectrum was obtained from the free induction decay (FID) at constant magnetic field following a single microwave pulse. The FID was Fourier transformed to give an absorption spectrum rather than the first derivative usually obtained in CW-EPR. The spectrum has been corrected for the response function of the spectrometer. Spin exchange with oxygen broadens all six spectral lines. However, spin exchange with other spin label molecules not only broadens lines but also produces incipient averaging of the proton hyperfine splitting. Thus, the measured proton splitting reports on the local spin label concentration, allowing the broadening to be corrected for exchange with spin labels. In addition, deuteration of most of the molecule has the advantage of reducing the inhomogeneous broadening, giving narrower, more intense lines. This is particularly beneficial for LF-EPR where first-derivative spectra are recorded.

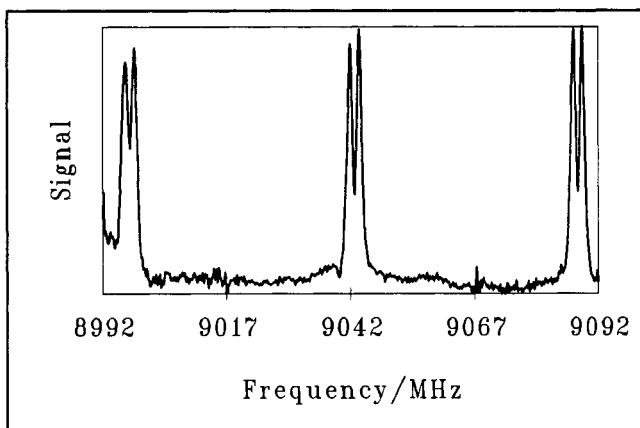


Fig. 4 FT-EPR spectrum of 0.15 mM aqueous solution of **3** at room temperature in a single-pulse experiment.

The central nitrogen hyperfine doublet in the LF-EPR spectrum of **3** changes noticeably in solutions of water equilibrated with molecular oxygen, Fig. 5. The two proton hyperfine lines broaden with increasing oxygen, overlapping more and more. The lineshape changes noticed in Fig. 5, are caused by a broadening of the two hyperfine lines with consequent loss of resolution. Such spectra were fit by a pair of Voigt lines, one for each of the proton hyperfine lines, using the techniques outlined above. In the fitting procedure, the shape and width are identical for both lines but the width and their splitting are varied to obtain the best fit. A third line can be introduced into the fitting procedure to account for a small amount of a fully deuterated impurity in **3**. This fitting employs information from the entire EPR line, not just from a few special points in the spectrum. This has the effect of increasing the "signal to noise ratio" of the measurement or fit since more of the EPR signal is included in the measurement of the linewidth parameters.

The spin relaxation rates are shown in Fig. 6 for several concentrations of spin label. The relaxation rate is linearly dependent on both oxygen concentration and spin label concentration. The relaxation rates are described by:

$$T_2^{-1} = 2.13 \times 10^6 \text{ s}^{-1} + 8.82 \times 10^9 \text{ M}^{-1} \text{ s}^{-1} [\text{O}_2] + 2.76 \times 10^9 \text{ M}^{-1} \text{ s}^{-1} [\mathbf{3}] \quad (1)$$

where the concentrations of molecular oxygen and spin label are given in mole per liter. The solid circles in Fig. 6 are from FT-EPR measurements on air-equilibrated aqueous samples and one degassed sample. A constant was added to these points in order to superimpose them on the data from the LF-EPR. The good overlap indicates that eqn. 1 also describes the data at X-band except for the leading, constant term which is $1.68 \times 10^6 \text{ s}^{-1}$. Label **3**, like **2**, has an intrinsic spin-spin relaxation rate that is greater

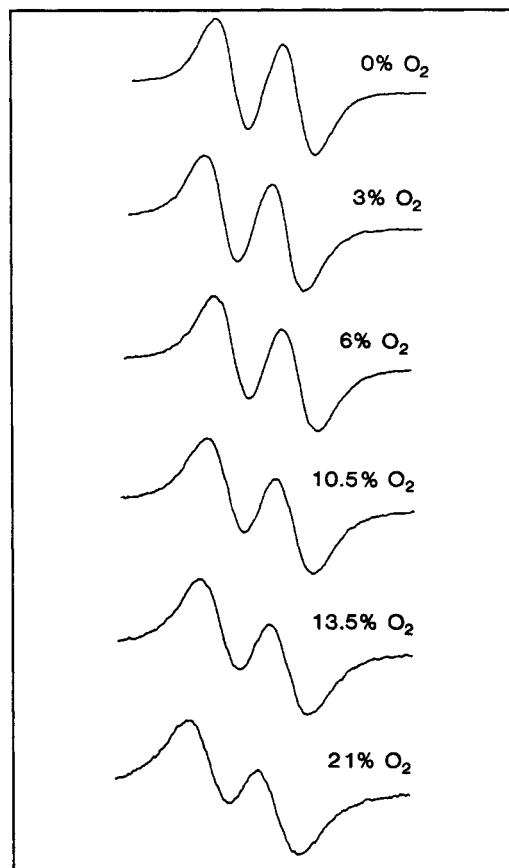


Fig. 5 LF-EPR spectra of **3** in water. Samples of 10 ml of 10^{-4} M spin label were equilibrated with 1 atm. of a mixture of nitrogen and oxygen.

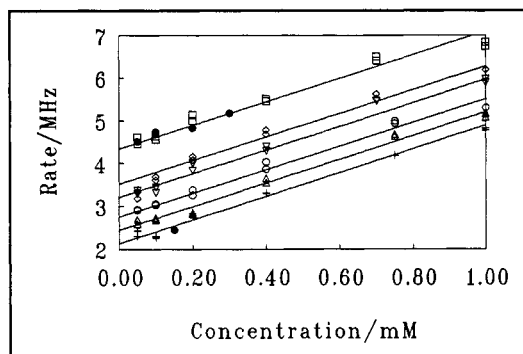


Fig. 6 Relaxation rates in water of **3** at room temperature. O_2 : + 0 mM, Δ 0.035 mM, \circ 0.07 mM, ∇ 0.122 mM, \times 0.157 mM, \blacksquare 0.25 mM for LF-EPR; \bullet FT-EPR at 0 mM and 0.25 mM.

at 250 MHz than at X-band. Spin exchange with oxygen and spin label affects the linewidth of this spin label equally at both frequencies and although the intrinsic

homogeneous broadening is slightly less at X-band, it does not improve the resolution of the proton hyperfine splitting.

Spin exchange with spin label decreases the proton hyperfine splitting in **3** as a result of incipient averaging of the two lines, Fig. 7. The straight line in the plot is a least-squares fit to the data. The splitting, S , is given by:

$$S = 0.0513 \text{ mT} - 3.6 \mu\text{T/mM} [3] \quad (2)$$

with the concentration given in millimolar units. The dependence of the splitting on oxygen concentration is too weak to be measured from this data and is at most 2% that for spin label. Thus, the splitting between the proton hyperfine lines can be used as a direct, linear measure of the local spin label concentration for levels encountered in *in vivo* oximetry.

FREQUENCY DEPENDENCE

When making EPR measurements at two very different frequencies, the results may not be directly comparable because of the frequency dependence of the spin properties that influence the spectrum. This is obvious in the case of a nitroxide in a solid where the g -factor anisotropy produces very different spectra at different frequencies. Even in the fast motional limit where the g -factor anisotropy is completely averaged, the g -factor anisotropy can still contribute to spin-lattice and spin-spin relaxation. Other interactions, such as dipolar interactions between radicals, have a dependence on EPR frequency or on differences of frequencies. Thus, it is not surprising that we find that the spin-spin relaxation rates for both **2** and **3** is different at 250 MHz and X-band. However, this does not mean that all contributions to the spin-spin relaxation rate vary with EPR frequency.

In the two spin labels we have examined here, the dependence of the relaxation rate on spin-label concentration and on oxygen concentration were the same at both EPR frequencies. If we use the simple model of relaxation caused by Heisenberg spin exchange, the rate constants are proportional to the rate of encounters between paramagnetic species in the samples. The encounter rates are clearly independent of EPR frequency and agrees with the lack of an experimentally measured frequency dependence. It means that spin exchange rates, in the fast motional limit, can be compared directly for measurements at different EPR frequencies, at least in the range 250-9100 MHz.

The intercept in Figs. 2 and 6, the intrinsic spin-spin relaxation rate, are frequency dependent. Simple considerations lead one to expect some of the contributions to this intercept, such as from rotational modulation of hyperfine interactions and from spin-rotation interaction, to be independent of frequency. Others, notably the rotational modulation of g -factor anisotropy, should be less effective as the EPR frequency (and magnetic field) are decreased. The experimental observations are just the opposite. The intrinsic spin-spin relaxation rate, at least in the two examples shown here, are actually larger at low frequency than at high frequency. This may result from a breakdown in some of the assumptions that are made when considering relaxation at X-band and which are no longer true at 250 MHz. In the case of the nitroxides, the high field approximation, which assumes that the external magnetic field is, by far, the largest interaction is starting to fail. In any event, the relaxation rates seem to vary slowly with EPR frequency. Spin labels developed for an application in the fast motional regime for one EPR frequency should be useful at other frequencies as well.

REFERENCES

1. R. N. Schwartz, L. L. Jones, and M. K. Bowman, *J. Phys. Chem.*, **83**, 3429-3434 (1979).
2. B. L. Bales, in *Biological Magnetic Resonance*, Vol. 8, Eds. L. J. Berliner and J. Reuben (Plenum, New York, 1989).
3. G. L. Millhauser and J. H. Freed, *J. Chem. Phys.*, **81**, 37 (1984).
4. L. Kar, G. L. Millhauser, and J. H. Freed, *J. Phys. Chem.*, **88**, 3951 (1984).
5. G. L. Millhauser, J. Gorchester, and J. H. Freed, in *Electronic Magnetic Resonance of the Solid State*, eds. J. A. Weil, M. K. Bowman, J. R. Morton, and K. F. Preston, (Canadian Chemical Society, Ottawa, 1987).
6. L. Kar, M. E. Johnson, and M. K. Bowman, *J. Magn. Reson.*, **75**, 397-413 (1987).
7. A. Angerhofer, M. Toporowicz, M. K. Bowman, J. R. Norris, and H. Levanon, *J. Phys. Chem.*, **92**, 7164-7166 (1988).
8. M. K. Bowman, M. Toporowicz, J. R. Norris, T. J. Michalski, A. Angerhofer, and H. Levanon, *Isr. J. Chem.*, **28**, 215-222 (1988).
9. G. B. Birrell, T. D. Lee, O. H. Griffith, J. W. Keana, *Bioorg. Chem.*, **7**, 409-420 (1978).
10. R. J. Massoth, Ph.D. Dissertation, University of Kansas, 1987.
11. A. Angerhofer, R. J. Massoth, and M. K. Bowman, *Isr. J. Chem.*, **28**, 227-238 (1988).
12. H. J. Halpern, D. P. Spencer, J. van Polen, M. K. Bowman, A. C. Nelson, E. M. Dowey, and B. A. Teicher, *Rev. Sci. Instr.*, **60**, 1080 (1989).
13. Y. A. Lin, B. A. Teicher, and H. J. Halpern, *J. Labelled Compds. Radiopharm.*, in press.
14. M. J. Povitch, *Analyt. Chem.*, **47**, 346 (1975).
15. J. M. Baker, V. G. Budker, S. I. Eremenko, and Yu. N. Molin, *Biochim. Biophys. Acta.*, **460**, 152 (1977).
16. C.-S. Lai, L. E. Hopwood, J. S. Hyde, and S. Lukiewicz, *Proc. Natl. Acad. Sci. USA.*, **79**, 1166 (1982).

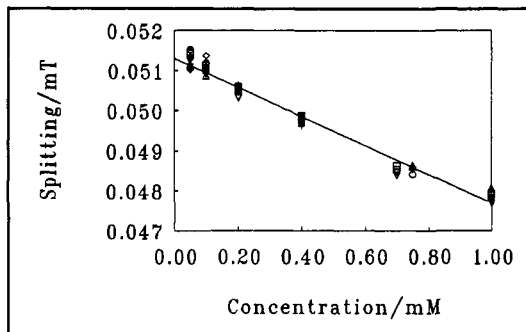


Fig. 7 Splitting of the proton hyperfine lines in **3**. Symbols are as in Fig. 6.